The liver-specific tumor suppressor STAT5 controls expression of the ROS generating enzyme NOX4 and the pro-apoptotic proteins PUMA and BIM

Ji Hoon Yu[1], **Bing-Mei Zhu**[2], **Gregory Riedlinger**[3], **Keunsoo Kang**[1], and **Lothar Hennighausen**[1,4]

[1]Laboratory of Genetics and Physiology, National Institute of Diabetes and Digestive and Kidney Diseases

[2]Key Laboratory of Acupuncture and Medicine Research of Ministry of Education, Nanjing University of Chinese Medicine, Nanjing, China, 210029

[3]Laboratory of Pathology, National Cancer Institute, National Institutes of Health, Bethesda, MD 20892, USA

[4]Department of Nanobiomedical Science and WCU Research Center of Nanobiomedical Science, Dankook University, Cheonan, Chungnam 330–714, Republic of Korea

Abstract

Loss of STAT5 from liver tissue results in hepatosteatosis and enhanced cell proliferation. This study now demonstrates that liver-specific *Stat5*-null mice develop severe hepatosteatosis as well as hepatocellular carcinomas at 17 months of age even in the absence of chemical insults. To understand STAT5's role as tumor suppressor we have identified and investigated new STAT5 target genes. Expression of *Nox4*, the gene encoding the Reactive Oxygen Species (ROS) generating enzyme NOX4, was induced by growth hormone through STAT5. In addition, the genes encoding the pro-apoptotic proteins PUMA and BIM were induced by growth hormone through STAT5, which bound to GAS motifs in the promoter regions of all three genes. We further show that STAT5-induced activation of *Puma* and *Bim* was dependent on NOX4. Treatment of mice with TGF-β, an inducer of apoptosis, resulted in cleaved caspase 3 in control but not in liver-specific *Stat5*-null mice. This study for the first time demonstrates that cytokines through STAT5 regulate the expression of the ROS generating enzyme NOX4 and key pro-apoptotic proteins. We propose that STAT5 harnesses several distinct signaling pathways in liver and thereby functions as a tumor suppressor. Besides suppressing the activation of STAT3, STAT5 induces the expression of pro-apoptotic genes and the production of ROS.

Keywords

STAT5; NOX4; PUMA; BIM; HCC

Introduction

Signal Transducers and Activators of Transcription (STAT) 5A and 5B are latent transcription factors that are induced by a plethora of cytokines, including growth hormone,

Address Correspondence to: Lothar Hennighausen, Laboratory of Genetics and Physiology, National Institute of Diabetes and Digestive and Kidney Diseases, National Institutes of Health, 8 Center Drive, Room 101, Bethesda, MD 20892-0822, tel. 301-496-2716, fax. 301-480-7312, lotharh@mail.nih.gov.

prolactin and several interleukins.[1] Recently, context-specific tumor suppressor functions have been associated with STAT5, such as inhibiting expression of NPM1-ALK[2] and suppressing STAT3 and TGF-β activity in liver.[3] Although active STAT5 has been detected in many human tumors, in normal cells constitutively active STAT5A induces senescence[4]. In particular, SOCS1 expression induced by aberrant STAT5 signaling can facilitate the process of cellular senescence, which is an important tumor suppressor mechanism[5].

Mice from which the *Stat5a/b* locus has been deleted specifically in liver tissue displayed altered metabolic pathways and developed fatty liver (nonalcoholic steatohepatitis).[6, 7] Treatment of these mice with CCl_4 led to liver fibrosis and hepatocellular carcinoma (HCC) suggesting that STAT5 is a tumor suppressor.[3] Aberrant activation of the TGF-β and STAT3 pathways in these mice appears to contribute to the CCl_4-induced fibrosis and HCC.[3]

Defects in apoptosis can be pivotal contributors to the development of cancer and the impaired response of tumor cells to therapy.[8] It is not clear to what extent STAT5 regulates apoptotic mechanism in liver tissue. The proapoptotic BH3-only proteins PUMA, BIM, and BID are essential for the activation of BAX- and BAK-dependent cell death programs.[9] PUMA expression is reduced in melanoma tumor tissue,[10] and loss of PUMA dramatically accelerated myc-induced lymphomagenesis in vivo.[11] Concomitant loss of PUMA and BIM in respective knock-out mice exacerbated hyperplasia of lymphatic organs, and promoted spontaneous malignancies.[12] Loss of PUMA- and BAX/BAK-dependent apoptosis also enhanced tumorigenesis in a hypoxia-induced tumor model.[13] In liver, JNK1-dependent PUMA expression induced hepatocyte lipoapoptosis.[14] Moreover, BIM and PUMA induction, and BAX activation by palmitate induced apoptosis in hepatocytes.[15] BIM and BID are critical contributors in hepatocyte apotosis caused by TNFα in vivo.[16] TNFα can cooperate with FasL to induce hepatocyte apoptosis by activating BIM and BID.[17] These results demonstrate that PUMA and BIM can function as tumor suppressors in mice.

Recent studies have demonstrated that NOX4 as a source of oxidative stress promotes apoptosis in vascular endothelial cell[18] and hepatocyte,[19] mitochondrial dysfunction in cardiac myocytes,[20,21] and cellular senescence in hepatocytes.[22]

In a quest to further understand STAT5's role as a liver-specific tumor suppressor we have identified novel STAT5 target genes in liver and mouse embryonic fibroblasts. This study for the first time explores the link between STAT5 and NOX4 and the apoptotic proteins PUMA and BIM.

Materials and Methods

Mice breeding

Stat5f/f;Alb-Cre mice were generated by breeding *Stat5f/f* mice with Alb-Cre transgenic mice.[23] *Stat5f/f* and Alb-Cre transgenic mice were on a mixed background. Only 8- to 68-week-old male mice were used in the experiments unless otherwise indicated. Animals were treated humanely and experiments and procedures were performed according to the protocol approved by the Animal Use and Care Committee at the National Institute of Diabetes and Digestive and Kidney Diseases.

Liver induced by CCl_4 or GH

Hepatic fibrosis in mice was induced by intraperitoneal (i.p.) injection with 2 ml/kg body weight of 10% CCl_4 (Sigma, St. Louis, MO) dissolved in olive oil (Sigma, St. Louis, MO), 3 times per week for 12 weeks. For growth hormone (GH) stimulation, mice were injected i.p.

with GH (2μg/g body weight) (mGH, NHPP, NIDDK). Four hours after injection mice were euthanized and livers were harvested for analyses.

Cell Culture

Mouse hepatocyte AML12 cells were obtained from ATCC (Manassas, VA) and cultured in a 1:1 mixture of Dulbecco's modified Eagle's medium (DMEM) and Ham's F12 medium supplemented with 10% fetal bovine serum (FBS), 5 μg/mL insulin, 5 μg/mL transferrin, 5 ng/mL selenium, and 40 ng/mL dexamethasone at 37°C with 5% CO_2.

Antibodies, immunoblotting and immunostaining

In brief, liver tissue was lysed by adding NuPAGE LDS Sample buffer (Invitrogen, Carlsbad, CA). Western blotting was performed according to the manufacturer's instructions (Invitrogen, Carlsbad, CA). The rabbit polyclonal anti-STAT5 (C-17), anti-STAT3 (C-20), anti-β-actin antibodies (Santa Cruz Biotechnology, Santa Cruz, CA), anti-phospho-STAT5, anti-phospho-STAT3 (Cell Signaling Technology, Beverly, MA), anti-NOX4 (Novus Biologicals, Littleton, CO), anti-PUMA (Abcam, Cambridge, MA) and anti-BIM (Cell Signaling Technology, Beverly, MA) were used for probing western blots. Immunohistochemistry was performed using standard procedures. In short, liver tissues were removed and fixed in 10% neutral buffered formalin and embedded in paraffin wax. Five μm sections were prepared for hematoxylin and eosin (H&E) staining and immunofluorescence analyses. After deparaffinization, antigen unmasking was performed in a Decloaking chamber (Biocare Medical, San Diego, CA) using BORG Decloaker Solution (Biocare Medical, San Diego, CA) for 5 min at 125°C. The sections were blocked for 30 min in TBS-T containing 3% goat serum. Primary antibodies used in this study included rabbit anti-phospho-STAT5 (Tyr694), anti-cleaved Caspase-3 (Cell Signaling Technology, Beverly, MA), rabbit anti-NOX4 (Novus Biologicals, Littleton, CO), rabbit anti-PUMA (Abcam, Cambridge, MA), anti-BIM (Cell Signaling Technology, Beverly, MA), anti-phospho-histone H3 (Upstate Biotechnology, Lake Placid, NY) and anti-Ki 67 (Santa Cruz Biotechnology, Santa Cruz, CA) in addition to mouse anti-β-catenin (BD Transduction Laboratories, San Jose, CA). For double-labeling immunofluorescence analyses, sections exposed to a pair of primary antibodies were incubated in a 1:400 dilution of goat anti-rabbit IgG conjugated with a red fluorophore (Alexa Fluor 594; Molecular Probes, Eugene, OR) and goat anti-mouse IgG conjugated with a green fluorophore (Alexa Fluor 488; Molecular Probes, Eugene, OR) for 30 min at room temperature. Images were obtained with a Retiga Exi camera on a Olympus BX51 microscope (Olympus America, Center Valley, PA) using Image-Pro 5.1 software.

Chromatin immunoprecipitation assay

For growth hormone (GH) stimulation, mice were injected with 2 μg/g body weight of GH by i.p. They were sacrificed 45 minutes after injection and liver tissue was harvested. Non-injected mice were used as controls. Liver tissue was cross-linked in 1.5% formaldehyde for 15 min at 37°C and sonicated using the Misonix Sonicator 3000 (Misonix, Farmingdale, NY, USA). Immunoprecipitation was carried out in TE buffer containing protease inhibitors (Sigma, St. Louis, MO). Chromatin was incubated with protein A Dynabeads (Invitrogen, Carlsbad, CA), which were pre-incubated with STAT5A or IgG antibody (R&D Systems, Minneapolis, MN, USA). Immunoprecipitated DNA was eluted and amplified by real-time PCR using a 7900 HT fast real-time PCR system (Applied Biosystems, Foster City, CA) and analyzed using SDS2.3 Software (Applied Biosystems, Foster City, CA). Sequence-specific primers used for amplification of the putative STAT5 binding sites (GAS sites) within the *Socs2, Nox4, Puma* and *Bim* genes were as following: For the *Socs2* GAS sequence, forward primer 5'-GGAGGGCGGAGTCGCAGGC-3', reverse primer 5'-GACTTGGCAAGAGTTAACCGTC-3'; the primer sets for *Nox4* gene were: GAS1,

forward 5'-AGGCTACTTCCGGCTCAAAT-3', reverse 5'-GCGCATACACCCTACTTCCT-3'; GAS2, forward 5'-CCCAATCAGGGCATACATTT-3', reverse 5'-TTTCCCATTCCTAGCACAGC-3'; the primer sets for *Puma* gene were: GAS1, forward 5'-AGCAGGAACCTGTCTCAGGA-3', reverse 5'-TAAAGGCTGACCCCTTCTCA-3'; the primer sets for *Bim* gene were: GAS1, forward 5'-GAAGAGGGGTGAGCATCTTG-3', reverse 5'-CAGTTGGAAGCCTCAGAAGG-3'; GAS2, forward 5'-GGGTCGGTACTGGCATCTAA-3', reverse 5'-GCTCGGCGTTAATCACTTTC-3'.

RNA isolation and quantitative real-time PCR analysis

Total RNA was isolated from liver tissue of *Stat5^f/f^, Stat5^f/f;Alb-Cre^* mice and hepatocytes using RNeasy mini kit (Qiagen, Valencia, CA) and one µg of RNA was reverse transcribed (cDNA reverse transcription kit; Applied Biosystems, Foster City, CA). Real-time quantification of mRNA transcript levels was performed using the TaqMan gene Expression Master Mix (Applied Biosystems, Foster City, CA) according to the manufacturer's instructions. Real-time PCR was carried out using an ABI Prism 7900HT (Applied Biosystems, Foster City, CA). TaqMan probes for *Nox4* (Mm00479246_m1), *Socs2* (Mm00850544_g1), *Puma* (Mm00519268_m1), *Bim* (Mm00437795_m1) and *beta-actin* (4352341E) were used (Applied Biosystems, Foster City, CA) for Real-time PCR. The SYBR primer were *Cdkn2b*, forward 5'-CCCTGCCACCCTTACCAGA-3', reverse 5'-CAGATACCTCGCAATGTCACG-3'; *GAPDH*, forward 5'-AACGACCCCTTCATTGAC-3', reverse 5'-TCCACGACATACTCAGCAC-3'.

Statistics

All statistical analyses were performed using the Student's *t* test (2 tailed, unpaired). A P value of 0.05 or less was considered significant.

Results

STAT5-dependent regulation of *Nox4, Puma* and *Bim* in liver tissue

In a quest to gain further insight into STAT5's role as tumor suppressor and understand underlying genetic pathways, we mined microarray-based expression data from liver tissue of control and liver-specific *Stat5*-null mice and from *Stat5^+/+^* and *Stat5^−/−^* mouse embryonic fibroblasts (MEFs) (for GEO accession numbers see Materials and Methods). In addition to the reduced expression of genuine STAT5 target genes, such as *Socs2*, in *Stat5*-null liver tissue we observed a 2.5- and 3.6-fold reduction of *Nox4 and Bim* mRNA levels, respectively (Supporting Table 1). Similarly, expression of *Nox4* in *Stat5^−/−^* MEFs was reduced 3.3-fold (Supporting Table 2). In addition, we observed a 5.7-fold reduction of *Puma* mRNA in *Stat5^−/−^* MEFs. While NOX4 (NADPH oxidase 4) is a reactive oxygen species (ROS) generating enzyme, BIM and PUMA are pro-apoptotic proteins. Quantitative RT-PCR and western blots confirmed GH- and STAT5-dependency of the *Nox4, Puma* and *Bim* genes in liver tissue. *Nox4, Puma* and *Bim* mRNA levels were reduced in *Stat5*-null livers (Fig. 1A). The *Socs2* gene served as a positive control (Fig. 1A,B). NOX4, PUMA and BIM protein concentrations were also reduced in *Stat5*-null livers (Fig. 1D). Actin served as a loading control and the greatly reduced STAT5 levels verified the efficient deletion of the *Stat5* locus. To establish GH-dependent expression *in vivo*, control and liver-specific *Stat5*-null mice were injected with GH followed by mRNA analyses. While GH treatment of control mice induced *Nox4* mRNA levels, no such increase was observed in the absence of STAT5 (Supporting Table 1, Fig. 1B).

To determine whether STAT5 directly binds to, and thereby controls the *Nox4* gene in liver, we scanned the promoter region for GAS motifs. ChIP analyses in *Stat5*-null livers

confirmed GH-induced STAT5 binding to two GAS motifs in the *Nox4* gene promoter (Fig. 1C). STAT5 binding to a GAS motif in the *Socs2* gene promoter served as a positive control (Fig. 1C).

Similar to *Nox4*, GH-induced *Puma* and *Bim* expression in liver tissue was STAT5 dependent (Fig. 2A) and STAT5 bound to GAS motifs in the respective promoter regions as determined by ChIP analyses (Fig. 2B). Binding to the *Socs2* gene promoter served as a positive control.

STAT5 does not control the anti-apoptotic genes *Bcl2, Bcl2l1* and *Mcl1*

To determine whether STAT5 also controls expression of anti-apoptotic genes, we analyzed mRNA levels of the *Bcl2, Bcl2l1* and *Mcl1* genes in control and *Stat5*-null livers. The respective mRNA levels did not change significantly in the absence of STAT5 suggesting that these genes are not under STAT5 control (Supporting Fig. 1A). Moreover, *Bcl2, Bcl2l1* and *Mcl1* mRNA levels did not change upon acute GH treatment of mice (Supporting Fig. 1B). We also explored direct STAT5 binding to the respective genomic loci in MEFs through ChIP-seq analyses. Although GAS motifs were identified in the *Bcl2, Bcl2l1* and *Mcl1* gene promoters, no significant STAT5 binding was observed (Supporting Fig. 1C). In addition, no binding was observed in the miR15/16 locus. Binding to the promoter-bound GAS motif in the *Socs2* gene served as a positive control.

Expression of *Nox4* in MEFs is under STAT5 control

To gain mechanistic insight into the STAT5 control of *Nox4*, *Puma* and *Bim* and their interrelationship, we resorted to $Stat5^{-/-}$ MEFs and $Stat5^{-/-}$ MEFs ectopically expressing STAT5A ($Stat5^{-/-}$; *Stat5A)* using a retroviral expression vector. This system also permitted us to study links between STAT5 and NOX4 promoted ROS production. Overexpression of STAT5A in $Stat5^{-/-}$ MEFs led to a further increase of *Nox4* and *Socs2* expression (Supporting Fig. 2A) and GH-induced expression of these genes was restored (Supporting Fig. 2B). STAT5-mediated induction of NOX4 was also observed at the protein level (Supporting Fig. 2E). To address whether the *Nox4* gene is under direct GH/STAT5 control, $Stat5^{+/+}$ and $Stat5^{-/-}$ MEFs were stimulated with GH. While *Nox4* expression was induced 1.9-fold in $Stat5^{+/+}$ MEFs, no induction was observed in $Stat5^{-/-}$ MEFs, (Supporting Fig. 3A). Similarly, *Socs2* gene expression was not stimulated by GH in $Stat5^{-/-}$ MEFs (Supporting Fig. 3A). ChIP assays confirmed that STAT5 binds to the conserved proximal GAS motifs in the *Nox4* gene promoter (Supporting Fig. 2C). STAT5 binding to the *Socs2* gene promoter served as a positive control. Western blot analyses confirmed the reduction of NOX4 in $Stat5^{-/-}$ MEFs (Supporting Fig. 2D). NOX4 and BIM levels were increased in $Stat5^{-/-}$; *Stat5A* MEFs as compared to parental $Stat5^{-/-}$ MEFs further supporting that STAT5 directly controls expression of these genes (Supporting Fig. 2E).

STAT5 controlled expression of *Puma and Bim*

Expression of *Puma and Bim* was STAT5-dependent and under GH control in MEFs (Supporting Fig. 3A). Western blot analyses confirmed the reduction of PUMA and BIM in $Stat5^{-/-}$ MEFs (Supporting Fig. 2D). Overexpression of STAT5A in $Stat5^{-/-}$ MEFs further increased *Puma* and *Bim* mRNA levels (Supporting Fig. 4A) and GH-dependent induction of *Puma* and *Bim* expression was observed in $Stat5^{-/-}$; *Stat5A but not in Stat5^{-/-}* MEFs carrying an empty control retrovirus (Supporting Fig. 4B). Tyrosine p-STAT5 was detected in GH stimulated $Stat5^{+/+}$ MEFs (Supporting Fig. 3C) and elevated levels were observed in $Stat5^{-/-}$; *Stat5A* MEFs (Supporting Fig. 3D). Levels of p-p53 were also increased in $Stat5^{-/-}$; *Stat5A* MEFs as compared to parental $Stat5^{-/-}$ MEFs (Supporting Fig. 2E). *Puma* as a p53 target gene might be regulated by STAT5/p53 signaling.

One GAS motif was identified at position -605 in the *Puma* gene and two conserved GAS motifs were identified at positions -3684, and -540 in the *Bim* gene (Supporting Fig. 4C). ChIP analyses in *Stat5$^{+/+}$* MEFs confirmed GH-induced STAT5 binding to these GAS motifs (Supporting Fig. 4C). Binding to the *Socs2* gene promoter served as a positive control.

To explore mechanistic links between p-p53 and expression of a subset of p53 target genes, we analyzed *Stat5$^{-/-}$* and *Stat5$^{-/-}$*; *Stat5A* MEFs. Expression of *Bax, Fas, Noxa and Ataf* was increased in *Stat5$^{-/-}$*; *Stat5A* MEFs compared to *Stat5$^{-/-}$* MEFs carrying an empty control retrovirus (Supporting Fig. 5). Expression of the *p53 gene* was not changed in *Stat5$^{-/-}$*; *Stat5A* MEFs compared to *Stat5$^{-/-}$* MEFs.

STAT5/NOX4-dependent regulation of ROS levels

To determine whether ROS generation is under direct STAT5/NOX4 control, *Stat5$^{+/+}$* and *Stat5$^{-/-}$* MEFs were cultured and assayed for ROS using DCF-DA and lucigenin. DCF fluorescence, an indicator of ROS, was stronger in *Stat5$^{+/+}$* MEFs than in *Stat5$^{-/-}$* MEFs ones (Supporting Fig. 6A). Treatment with H_2O_2 further increased the production of ROS in *Stat5$^{+/+}$* MEFs, as compared to *Stat5$^{-/-}$* MEFs (Supporting Figs. 6A,7A). The Lucigenin chemiluminescent assays established that STAT5 deficiency led to a reduced level of intracellular ROS in MEFs (Supporting Fig. 6B). Treatment of *Stat5$^{+/+}$* MEFs with diphenylene iodonium (DPI), a NOX inhibitor, reduced ROS levels (Supporting Fig. 6A, 7B). Although DPI inhibits several NOX members, NOX4 is the only one expressed at appreciable levels in liver tissue. This suggests that ROS in MEFs originates from NOX4.

Puma and *Bim are* regulated by NOX4

To explore mechanistic links between STAT5A and NOX4 and expression of the *Puma* and *Bim* genes, we analyzed *Stat5$^{-/-}$* MEFs in the absence and presence of retrovirally introduced STAT5 (*Stat5$^{-/-}$*; *Stat5A*). Upon treatment of MEFs with DPI, expression of *Puma* and *Bim* was reduced only in MEFs expressing STAT5A (Supporting Fig. 6C). These data provide evidence that the *Puma* and *Bim* genes are regulated by STAT5 through NOX4 signaling. STAT5A-induced expression of the *Cdkn2b* gene, encoding a cell cycle inhibitor p15^{INK4B}, was partially suppressed in the presence of DPI (Supporting Fig. 8A, B) suggesting the STAT5-target *Cdkn2b* is also under NOX4 control.

Treatment of MEFs with H_2O_2 further induced *Puma mRNA* levels in the presence of STAT5A but not in the absence of STAT5 (Supporting Fig. 6D). Simultaneous treatment with DPI led to a suppression of *Puma* expression (Supporting Fig. 6D). Cell survival in the presence of H_2O_2 was less affected in the absence of STAT5 (Supporting Fig. 6E). Simultaneous treatment with DPI led to a rebound of cell survival in the presence of STAT5A and to a lesser extent in the absence of STAT5 (Supporting Fig. 6E). These data suggest that STAT5/NOX4 signaling in MEFs controlled PUMA-induced apoptosis and p15^{INK4B}-regulated cell cycle inhibition.

Puma and Bim are regulated by NOX4 in hepatocytes

To explore a possible relationship between STAT5/NOX4 and the *Puma and Bim* genes in hepatocytes, the cell line AML12 was treated with the NOX inhibitor DPI. This resulted in reduced levels of *Puma and Bim* mRNA (Fig. 2C). DPI treatment also resulted in decreased *Cdkn2b* expression. However, it did not change expression of the STAT5 target gene *Socs2*. Although DPI inhibits several NOX members, NOX4 is the only one family member expressed at appreciable levels in hepatocytes.[24] These data imply that the direct STAT5 target gene *Cdkn2b* is also regulated by STAT5/NOX4 signaling.

As shown above, STAT5 did not bind to the *Bcl2, Bcl2l1* and *Mcl1* gene loci and expression was not controlled by STAT5 (Supporting Fig. 1A–C). To test whether these anti-apoptotic genes were regulated by NOX4, AML12 hepatocytes were treated with the NOX inhibitor DPI. Expression of *Bcl2, Bcl2l1* and *Mcl1* was similar in treated and untreated cells (Supporting Fig. 1D), suggesting that these genes are not under STAT5/NOX4 control.

Immunohistochemistry was used as an independent means to corroborate the importance of STAT5 on the accumulation of NOX4, PUMA and BIM. NOX4, PUMA and BIM were observed in liver tissue of control mice (Fig. 3B–D, left panels) and at lower levels in liver-specific *Stat5*-null mice (Fig. 3B–D, right panels). GH-induced nuclear phospho-STAT5 staining was observed in control mice but not in the absence of STAT5 (Fig. 3A).

STAT5-dependent regulation of hepatoprotective proteins

Since loss of STAT5 is correlated with the development of liver disease it is possible that STAT5 promotes the expression of hepatoprotective genes. We therefore analyzed whether the hepatoprotective genes *Hnf6, Lifr, Egfr* and *Prlr* were under GH/STAT5 control. While GH treatment of control mice induced *Hnf6, Lifr, Egfr* and *Prlr* mRNA levels, no such increase was observed in the absence of STAT5 (Supporting Fig. 9). Expression of *Hnf6, Lifr, Egfr* and *Prlr* mRNA was slightly, yet not significantly, reduced in liver-specific *Stat5*-null mice (Supporting Fig. 9). Thus, reduced levels of hepatoprotective proteins may contribute to the development of liver disease in liver-specific *Stat5*-null mice.

Loss of STAT5 promotes the development of HCC in liver-specific *Stat5*-null mice

We had shown earlier that loss of STAT5 from liver tissue resulted in hepatosteatosis and HCC upon CCl_4 exposure in 3 months old mice.[3,25] To investigate whether loss of STAT5 can lead to the development of HCC without chemical injury, we analyzed control and liver-specific *Stat5*-null mice at 17 months of age. Severe heptosteatosis and HCC were observed in all four experimental mice analyzed but not in age-matched controls (Fig. 4, 5) and nodules were observed in two of the four mice. To investigate molecular consequences associated with the development of HCC, we analyzed p-STAT5 and p-STAT3 levels in control and liver-specific *Stat5*-null mice at 17 months of age. P-STAT3 levels were greatly elevated in liver-specific *Stat5*-null mice at 17 months of age (Fig. 4C) but not at 2 months. To determine whether loss of STAT5 correlated with increased cell proliferation, tissue sections were stained for phosphorylated histone H3 as a measure of cell proliferation (Fig. 5D). The number of phospho-Histone H3 positive nuclei in liver-specific Stat5-null mice at 17 months was higher than in age-matched controls.

As expected, levels of *Nox4, Puma, Bim* and *Socs2* mRNA were reduced in 17 months old liver-specific *Stat5*-null mice compared to age matched controls (Supporting Fig. 10A). In contrast, and as expected, *Bcl2l1* and *Mcl1* mRNA levels were not altered (Supporting Fig. 10B). Unexpectedly, *Bcl2* mRNA levels were increased in experimental mice (Supporting Fig. 10B).

CCl_4 treatment results in STAT5-dependent increase of *Puma* and *Bim*

To further investigate whether CCl_4 treatment contributes to the deregulation of *Nox4, Puma* and *Bim* we analyzed control and liver-specific *Stat5*-null mice at 3 months of age. CCl_4 treatment induced *Puma and Bim* mRNA levels in control mice but not in liver-specific *Stat5*-null mice (Supporting Fig. 11). In contrast, no change of *Nox4* expression was observed.

Using immunohistochemistry NOX4, PUMA and BIM were detected in liver tissue of control mice both in the absence and presence of CCl_4 (Fig. 6A–C). In contrast, reduced

NOX4, PUMA and BIM staining was observed in liver-specific *Stat5*-null mice in the absence and presence of CCl$_4$ (Fig. 6A–C).

To establish whether loss of STAT5 and reduced levels of PUMA and BIM correlated with increased cell proliferation, we stained tissue sections for Ki-67 as a measure of cell proliferation (Fig. 7A). The number of Ki-67 positive cells increased in liver tissue of liver-specific *Stat5*-null mice that had been treated with CCl$_4$ (Fig. 7A). In addition, activation of the apoptotic marker cleaved caspase-3 was decreased in liver tissue of *Stat5*-null mice treated with CCl$_4$ compared to treated control mice (Fig. 7B). Levels of the pro-apoptotic protein BAX were decreased in liver tissue from *Stat5*-null mice compared to control mice (Supporting Fig. 12A,B). Proliferating cell nuclear antigen (PCNA), an indicator of cell proliferation, concentrations were elevated in liver-specific *Stat5*-null mice treated with CCl$_4$ (Supporting Fig. 13A,B).

STAT5/NOX4-dependent regulation of apoptosis signaling in liver

To establish GH or TGF-β-dependent apoptosis signaling *in vivo*, control mice were injected with GH or TGF-β followed by protein and mRNA analyses. While GH treatment of control mice induced caspase3 activation and expression of *Nox4, Puma* and *Bim*, no such increase was observed in the absence of GH (Supporting Fig. 14A). TGF-β treatment of control mice, but not experimental mice, induced caspase3 activation and expression of *Nox4, Puma* and *Bim* mRNA levels (Supporting Fig. 14B). This suggests that caspase3 activation and expression of *Puma* and *Bim* by GH or TGF-β treatment induced apoptosis by STAT5/NOX4.

Discussion

While in many cell types the transcription factor STAT5 provides proliferative and survival cues by activating respective genetic programs, it serves as a bona fide tumor suppressor in liver tissue.[3,25] Loss of STAT5 from liver tissue leads to hepatosteatosis and the development of HCC upon CCl$_4$ treatment. In part STAT5's function as tumor suppressor can be attributed to its ability to regulate the cell cycle control genes *Cdkn2b* and *Cdkn1a*.[25] In addition, the presence of STAT5 also suppresses inappropriate cytokine-induced activation of STAT3, an oncoprotein in its own right.

We now provide evidence for additional venues used by STAT5 to control cell death and thus suppress the development of hepatocellular carcinoma. While CCl$_4$ exposure is required to induce HCC in 3 months-old liver-specific *Stat5*-null mice, 17 months-old mice develop HCC in the absence of this chemical insult. Thus, loss of STAT5 by itself is sufficient to fundamentally alter cellular metabolism conducive to disease development. In this study we have identified and investigated additional STAT5 target genes whose deregulation likely contribute to the development of HCC in the absence of STAT5. Notably, STAT5 controls ROS production through the activation of the *Nox4* gene and it activates the genes encoding the pro-apoptotic and tumor suppressive proteins PUMA and BIM. We therefore propose that STAT5 protects hepatocytes through several pathways, including the activation of cell death programs executed by NOX4, PUMA and BIM.

Studies on mice from which the genes encoding NOX4, PUMA and BIM had been deleted, as well as tissue culture cells expressing reduced levels of these proteins, provided sound evidence for these proteins in cell death programs. In hepatocytes, NOX4 is required for TGF-β -induced apoptosis[19] and loss of NOX4 from lung epithelium is protective from TGF-β-induced apoptosis.[26] In heart tissue, NOX4 protected cells from pressure overload-induced apoptosis.[20] In addition to NOX4, NOX1 and NOX2 have also been linked to cell death in hepatocytes, as CCl$_4$-dependent hepatic fibrosis and ROS generation were

attenuated in the absence of the latter two isoforms.[24,27,28] In addition BIM was also required for tumor cell apoptosis induced by a VEGF-A antagonist.[29] Roles for BIM and PUMA in suppressing oncogenesis have been described for B cell leukemias[30] and intestinal cells,[31,32] respectively. In those cases, BIM and PUMA exerted a strong apoptotic effect and their loss lead to enhanced tumorigenesis.

While STAT5 directly controls the expression of p15^{INK4B},[25] PUMA and BIM (Fig. 8), it can also exert its function through activating another direct downstream target gene *Nox4*, which encodes NADPH oxidase 4, a key regulator of ROS.[18,20] We further provide evidence for a direct link between NOX4 and PUMA and BIM. Inhibiting NOX4 activity led to decreased expression of PUMA and BIM and p15^{INK4B}. The mechanism of this regulatory venue is still elusive.

A picture is evolving that distinct signaling pathways emerging from STAT5 contribute to the protection of hepatocytes (Fig. 8). Hyperactive GH signaling imposed by a GH transgene promoted inflammatory liver cancer in mice and loss of STAT5 in these mice resulted in accelerated HCC.[33] This study linked STAT5 to hepatoprotective genes and the aberrant activation of c-Jun in the absence of STAT5. Moreover, the combined loss of STAT5 and the glucocorticoid receptor (GR) resulted in the development of frank HCC.[34] In that study development of HCC was associated with GH and insulin resistance and high ROS levels. Since NOX4, the enzyme generating ROS, is under STAT5 control, the source of ROS in the STAT5-GR double knock-out mice needs to be identified.

Although loss of STAT5 is sufficient to induce hepatosteatosis and HCC, it is not clear to what extent the loss of individual STAT5 executors, (NOX4, PUMA, BIM, p15^{INK4B}) would sensitize hepatocytes to injury and lead to pathological changes. Lastly, the molecular basis of STAT5's cell specificity, promoting proliferation in the hematopoietic system and apoptosis in liver, remains an enigma. Although STAT5 can activate genes controlling cell proliferation, survival and death, it is fair to propose that the relative activity of these pathways will determine whether STAT5 is an oncoprotein or a tumor suppressor.

Supplementary Material

Refer to Web version on PubMed Central for supplementary material.

Acknowledgments

References

1. Hennighausen L, Robinson GW. Interpretation of cytokine signaling through the transcription factors STAT5A and STAT5B. Genes Dev. 2008; 22:711–721. [PubMed: 18347089]

2. Zhang Q, Wang HY, Liu X, Wasik MA. STAT5A is epigenetically silenced by the tyrosine kinase NPM1-ALK and acts as a tumor suppressor by reciprocally inhibiting NPM1-ALK expression. Nat Med. 2007; 13:1341–1348. [PubMed: 17922009]

3. Hosui A, Kimura A, Yamaji D, Zhu BM, Na R, Hennighausen L. Loss of STAT5 causes liver fibrosis and cancer development through increased TGF-beta and STAT3 activation. J Exp Med. 2009; 206:819–831. [PubMed: 19332876]

4. Mallette FA, Gaumont-Leclerc MF, Ferbeyre G. The DNA damage signaling pathway is a critical mediator of oncogene-induced senescence. Genes Dev. 2007; 21:43–48. [PubMed: 17210786]

5. Calabrese V, Mallette FA, Deschenes-Simard X, Ramanathan S, Gagnon J, Moores A, et al. SOCS1 links cytokine signaling to p53 and senescence. Mol Cell. 2009; 36:754–767. [PubMed: 20005840]

6. Cui Y, Hosui A, Sun R, Shen K, Gavrilova O, Chen W, et al. Loss of signal transducer and activator of transcription 5 leads to hepatosteatosis and impaired liver regeneration. Hepatology. 2007; 46:504–513. [PubMed: 17640041]

7. Holloway MG, Cui Y, Laz EV, Hosui A, Hennighausen L, Waxman DJ. Loss of sexually dimorphic liver gene expression upon hepatocyte-specific deletion of Stat5a-Stat5b locus. Endocrinology. 2007; 148:1977–1986. [PubMed: 17317776]

8. Adams JM, Cory S. The Bcl-2 apoptotic switch in cancer development and therapy. Oncogene. 2007; 26:1324–1337. [PubMed: 17322918]

9. Ren D, Tu HC, Kim H, Wang GX, Bean GR, Takeuchi O, et al. BID, BIM, and PUMA are essential for activation of the BAX- and BAK-dependent cell death program. Science. 2010; 330:1390–1393. [PubMed: 21127253]

10. Karst AM, Dai DL, Martinka M, Li G. PUMA expression is significantly reduced in human cutaneous melanomas. Oncogene. 2005; 24:1111–1116. [PubMed: 15690057]

11. Hemann MT, Zilfou JT, Zhao Z, Burgess DJ, Hannon GJ, Lowe SW. Suppression of tumorigenesis by the p53 target PUMA. Proc Natl Acad Sci USA. 2004; 101:9333–9338. [PubMed: 15192153]

12. Erlacher M, Labi V, Manzl C, Bock G, Tzankov A, Hacker G, et al. Puma cooperates with Bim, the rate-limiting BH3-only protein in cell death during lymphocyte development, in apoptosis induction. J Exp Med. 2006; 203:2939–2951. [PubMed: 17178918]

13. Nelson DA, Tan TT, Rabson AB, Anderson D, Degenhardt K, White E. Hypoxia and defective apoptosis drive genomic instability and tumorigenesis. Genes Dev. 2004; 18:2095–2107. [PubMed: 15314031]

14. Cazanave SC, Mott JL, Elmi NA, Bronk SF, Werneburg NW, Akazawa Y, et al. JNK1-dependent PUMA Expression Contributes to Hepatocyte Lipoapoptosis. J Biol Chem. 2009; 284:26591–26602. [PubMed: 19638343]

15. Akazawa Y, Cazanave S, Mott JL, Elmi N, Bronk SF, Kohno S, et al. Palmitoleate attenuates palmitate-induced Bim and PUMA up-regulation and hepatocyte lipoapoptosis. J Hepatol. 2010; 52:586–593. [PubMed: 20206402]

16. Kaufmann T, Jost PJ, Pellegrini M, Puthalakath H, Gugasyan R, Gerondakis S, et al. Fatal Hepatitis Mediated by Tumor Necrosis Factor TNFα Requires Caspase-8 and Involves the BH3-Only Proteins Bid and Bim. Immunity. 2009; 30:56–66. [PubMed: 19119023]

17. Schmich K, Schlatter R, Corazza N, Sá Ferreira K, Ederer M, Brunner T, et al. Tumor necrosis factor α sensitizes primary murine hepatocytes to Fas/CD95-induced apoptosis in a Bim- and Bid-dependent manner. Hepatology. 2011; 53:282–292. [PubMed: 20872776]

18. Basuroy S, Tcheranova D, Bhattacharya S, Leffler CW, Parfenova H. Nox4 NADPH oxidase-derived reactive oxygen species, via endogenous carbon monoxide, promote survival of brain endothelial cells during TNF-α-induced apoptosis. Am J Physiol Cell Physiol. 2011; 300:C256–C265. [PubMed: 21123734]

19. Carmona-Cuenca I, Roncero C, Sancho P, Caja L, Fausto N, Fernández M, et al. Upregulation of the NADPH oxidase NOX4 by TGF-beta in hepatocytes is required for its pro-apoptotic activity. J Hepatol. 2008; 49:965–976. [PubMed: 18845355]

20. Kuroda J, Ago T, Matsushima S, Zhai P, Schneider MD, Sadoshima J. NADPH oxidase 4 (Nox4) is a major source of oxidative stress in the failing heart. Proc Natl Acad Sci U S A. 2010; 107:15565–15570. [PubMed: 20713697]

21. Ago T, Kuroda J, Pain J, Fu C, Li H, Sadoshima J. Upregulation of Nox4 by hypertrophic stimuli promotes apoptosis and mitochondrial dysfunction in cardiac myocytes. Circ Res. 2010; 106:1253–1264. [PubMed: 20185797]

22. Senturk S, Mumcuoglu M, Gursoy-Yuzugullu O, Cingoz B, Akcali KC, Ozturk M. Transforming growth factor-beta induces senescence in hepatocellular carcinoma cells and inhibits tumor growth. Hepatology. 2010; 52:966–974. [PubMed: 20583212]

23. Yakar S, Liu JL, Stannard B, Butler A, Accili D, Sauer B, et al. Normal growth and development in the absence of hepatic insulin-like growth factor I. Proc Natl Acad Sci U S A. 1999; 96:7324–7329. [PubMed: 10377413]

24. Paik YH, Iwaisako K, Seki E, Inokuchi S, Schnabl B, Osterreicher CH, et al. The nicotinamide adenine dinucleotide phosphate oxidase (NOX) homologues NOX1 and NOX2/gp91(phox) mediate hepatic fibrosis in mice. Hepatology. 2011; 53:1730–1741. [PubMed: 21384410]

25. Yu JH, Zhu BM, Wickre M, Riedlinger G, Chen W, Hosui A, et al. The transcription factors signal transducer and activator of transcription 5A (STAT5A) and STAT5B negatively regulate cell proliferation through the activation of cyclin-dependent kinase inhibitor 2b (Cdkn2b) and Cdkn1a expression. Hepatology. 2010; 52:1808–1818. [PubMed: 21038417]

26. Carnesecchi S, Deffert C, Donati Y, Basset O, Hinz B, Preynat-Seauve O, et al. A key role for NOX4 in epithelial cell death during development of lung fibrosis. Antioxid Redox Signal. 2011; 15:607–619. [PubMed: 21391892]

27. Jiang JX, Venugopal S, Serizawa N, Chen X, Scott F, Li Y, et al. Reduced nicotinamide adenine dinucleotide phosphate oxidase 2 plays a key role in stellate cell activation and liver fibrogenesis in vivo. Gastroenterology. 2010; 139:1375–1384. [PubMed: 20685364]

28. Cui W, Matsuno K, Iwata K, Ibi M, Matsumoto M, Zhang J, et al. NOX1/nicotinamide adenine dinucleotide phosphate, reduced form (NADPH) oxidase promotes proliferation of stellate cells and aggravates liver fibrosis induced by bile duct ligation. Hepatology. 2011; 54:949–958. [PubMed: 21618578]

29. Naik E, O'Reilly LA, Asselin-Labat ML, Merino D, Lin A, Cook M, et al. Destruction of tumor vasculature and abated tumor growth upon VEGF blockade is driven by proapoptotic protein Bim in endothelial cells. J Exp Med. 2011; 208:1351–1358. [PubMed: 21646395]

30. Egle A, Harris AW, Bouillet P, Cory S. Bim is a suppressor of Myc-induced mouse B cell leukemia. Proc Natl Acad Sci U S A. 2004; 101:6164–6169. [PubMed: 15079075]

31. Qiu W, Wu B, Wang X, Buchanan ME, Regueiro MD, Hartman DJ, et al. PUMA-mediated intestinal epithelial apoptosis contributes to ulcerative colitis in humans and mice. J Clin Invest. 2011; 121:1722–1732. [PubMed: 21490394]

32. Qiu W, Carson-Walter EB, Kuan SF, Zhang L, Yu J. PUMA suppresses intestinal tumorigenesis in mice. Cancer Res. 2009; 69:4999–5006. [PubMed: 19491259]

33. Friedbichler K, Themanns M, Mueller KM, Schlederer M, Kornfeld JW, Terracciano LM, et al. Growth-hormone-induced signal transducer and activator of transcription 5 signaling causes gigantism, inflammation, and premature death but protects mice from aggressive liver cancer. Hepatology. 2012; 55:941–952. [PubMed: 22031092]

34. Mueller KM, Kornfeld JW, Friedbichler K, Blaas L, Egger G, Esterbauer H, et al. Impairment of hepatic growth hormone and glucocorticoid receptor signaling causes steatosis and hepatocellular carcinoma in mice. Hepatology. 2011; 54:1398–1409. [PubMed: 21725989]
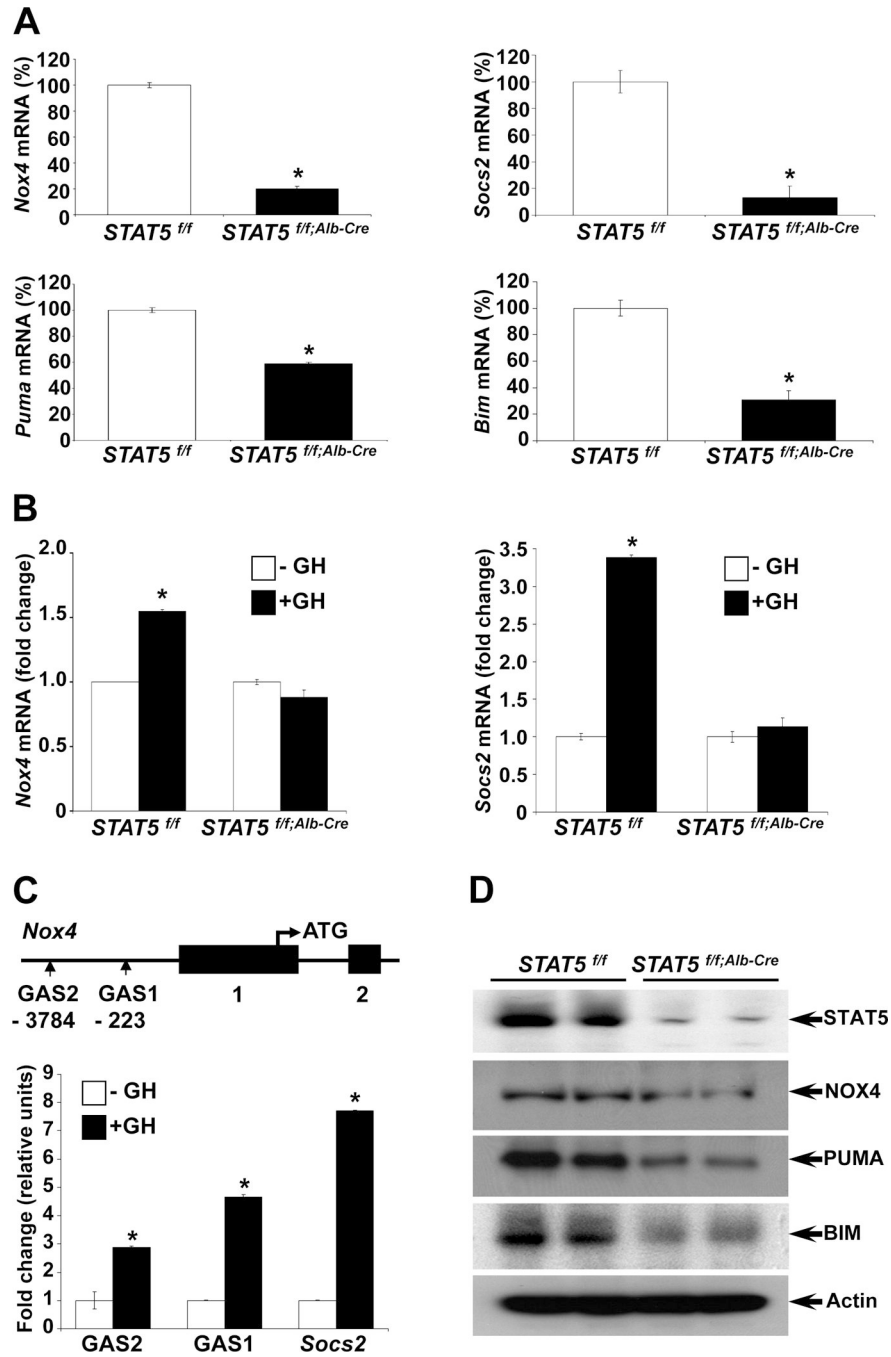
Figure 1.
STAT5 regulates *Nox4* expression through STAT5 binding to conserved GAS sites in the *Nox4* gene promoter in liver. (A) Expression of *Nox4*, *Puma*, *Bim* and *Socs2* was analyzed by quantitative real-time PCR in liver tissue from *Stat5^{f/f}* and *Stat5^{f/f;Alb-Cre}* mice. Values are shown as means ± SD. (B) mRNA expression of *Nox4* and *Socs2* in *Stat5^{f/f}* and *Stat5^{f/f;Alb-Cre}* mice. Mice were injected with GH, tissue was harvested after four hours and RNA was analyzed by quantitative real-time PCR. All values represent means ± SD. (C) Schematic of the *Nox4* gene. Vertical boxes indicate exons and conserved GAS sequences are marked. Chromatin immunoprecipitation (ChIP) analysis of STAT5 binding to the putative GAS sites. *Stat5^{f/f}* mice were injected with GH, tissue was harvested after 45

minutes and binding to GAS sites was analyzed by quantitative real-time PCR. DNA was amplified from STAT5-precipitated complexes using specific primers spanning GAS motifs in the *Socs2* and *Nox4* genes. All values represent means ± SD from 3 independent experiments performed in triplicates. (D) Levels of NOX4, PUMA and BIM in liver tissue from *Stat5$^{f/f}$* and *Stat5$^{f/f;Alb-Cre}$* mice. Expression of NOX4, PUMA and BIM was determined by western blotting. *P < .05; compared with corresponding controls.
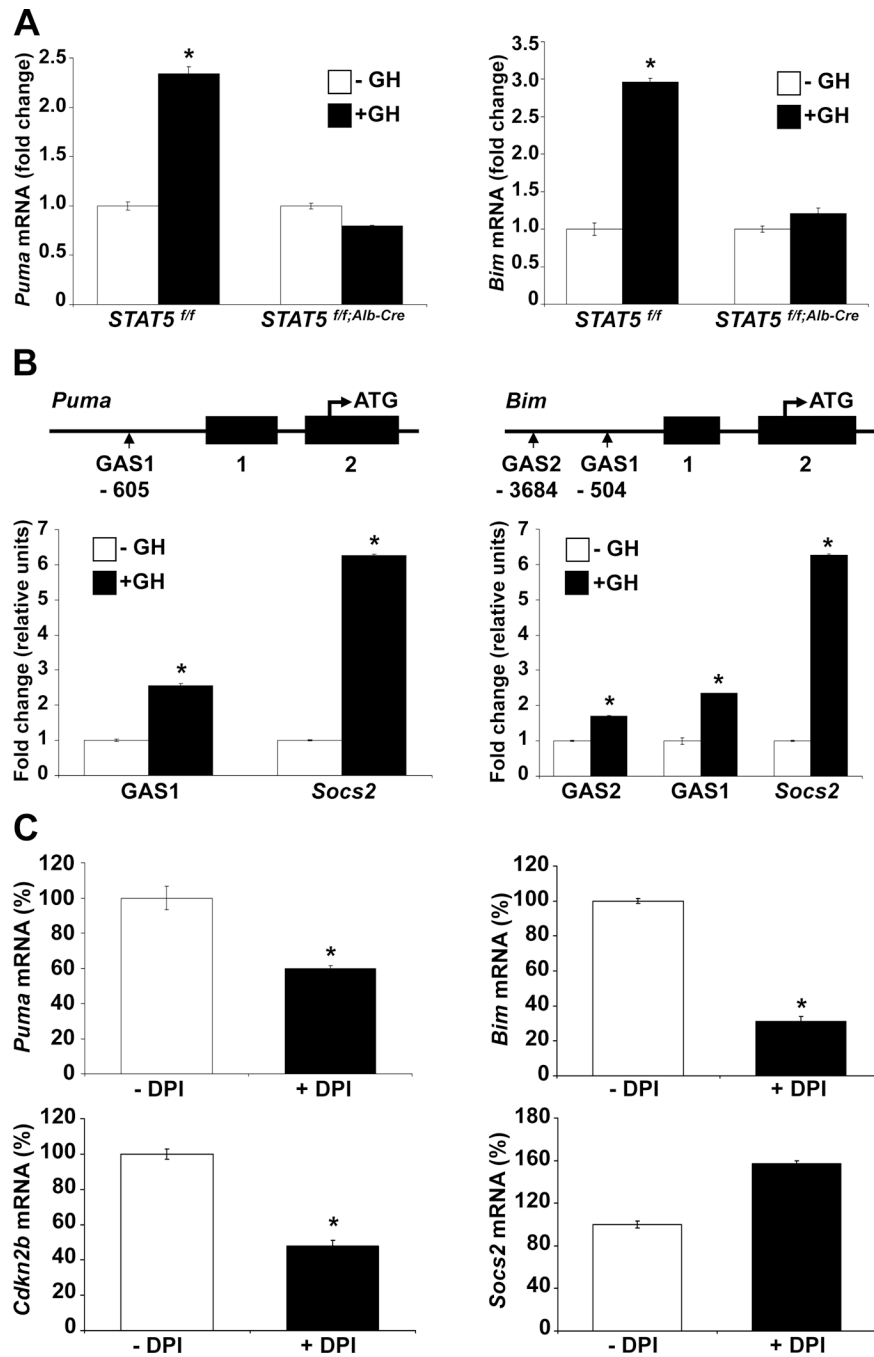
Figure 2.
STAT5 regulates expression of *Puma* and *Bim* through STAT5 binding to GAS sites in the *Puma* and *Bim* gene promoters in liver. (A) mRNA expression of *Puma* and *Bim* in *Stat5*$^{f/f}$ and *Stat5*$^{f/f;Alb-Cre}$ mice injected with GH. Mice were injected with GH and tissue was harvested after 4 hours. Expression of *Puma* and *Bim* was analyzed by quantitative real-time PCR in liver tissue from *Stat5*$^{f/f}$ and *Stat5*$^{f/f;Alb-Cre}$ mice. All values represent means ± SD. (B) Schematic of the *Puma* and *Bim* genes. Vertical boxes indicate exons and the location of conserved GAS sequences is shown. Chromatin immunoprecipitation (ChIP) analysis of STAT5 binding to the putative GAS sites. *Stat5*$^{f/f}$ mice were treated with GH and tissue was harvested after 45 minutes. Binding to GAS sites was analyzed by quantitative real-time

PCR. DNA was amplified from STAT5-precipitated complexes using specific primers for known (*Socs2*) and suspected (*Puma* and *Bim*) GAS regions. All values represent means ± SD from 3 independent experiments performed in triplicates. (C) mRNA expression of *Puma, Bim, Cdkn2b* and *Socs2* in immortalized wildtype hepatocyte of murine origin. The cells were treated with DPI for 2 hours. Expression of *Puma, Bim, Cdkn2b* and *Socs2* mRNA was analyzed by quantitative real-time PCR. All values represent means ± SD from 3 independent experiments. *P < .05; compared with corresponding controls.
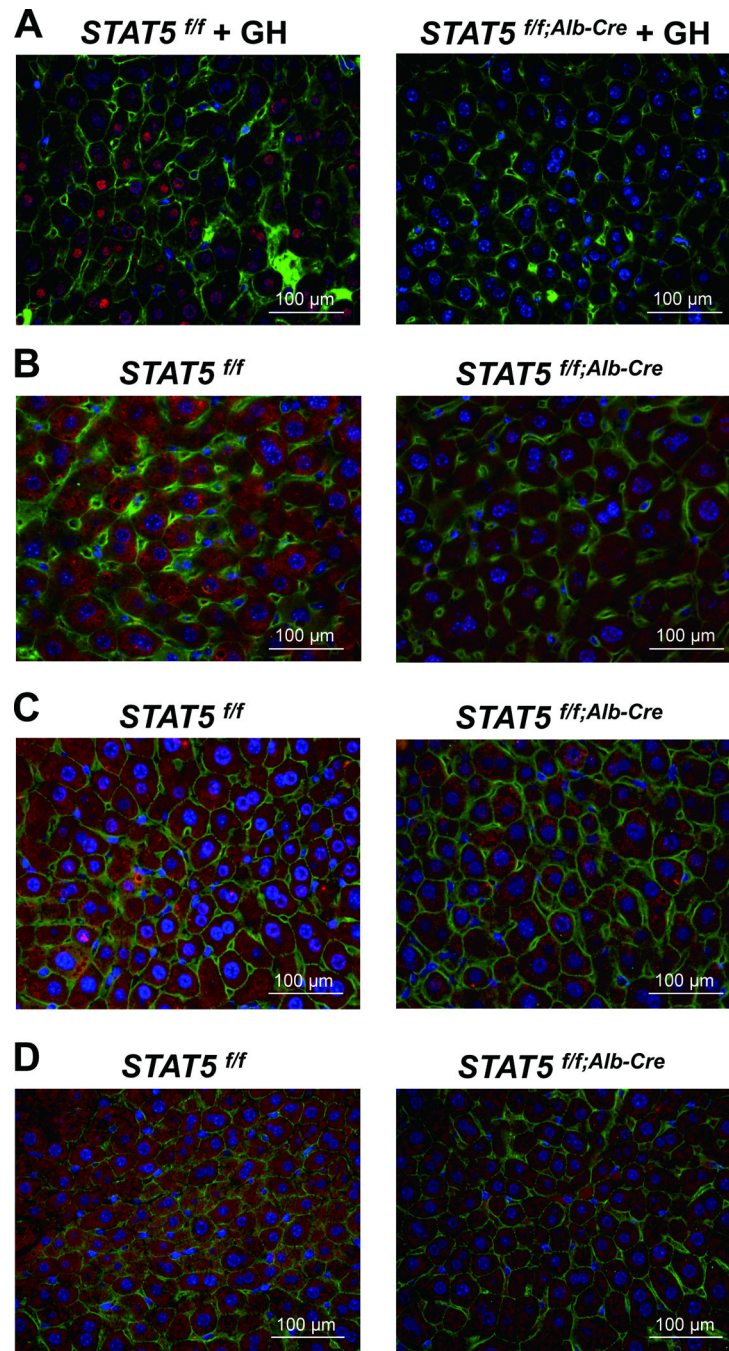
Figure 3.
Immunostaining of phospho-STAT5, NOX4, PUMA and BIM in *Stat5^f/f* and *Stat5^f/f;Alb-Cre* mice. (A) Livers from *Stat5^f/f* and *Stat5^f/f;Alb-Cre* mice were harvested after GH injection and analyzed for p-STAT5 expression using immunofluorescence staining with anti-p-STAT5 (red), anti-β-catenin (green) antibodies and DAPI (blue). (B–D) Livers from *Stat5^f/f and Stat5^f/f;Alb-Cre* mice were harvested and analyzed for NOX4 (B), PUMA (C) and BIM (D) expression using immunofluorescence staining with anti-NOX4 (red), anti-PUMA (red), anti-BIM (red), anti-β-catenin (green) antibodies and DAPI (blue).
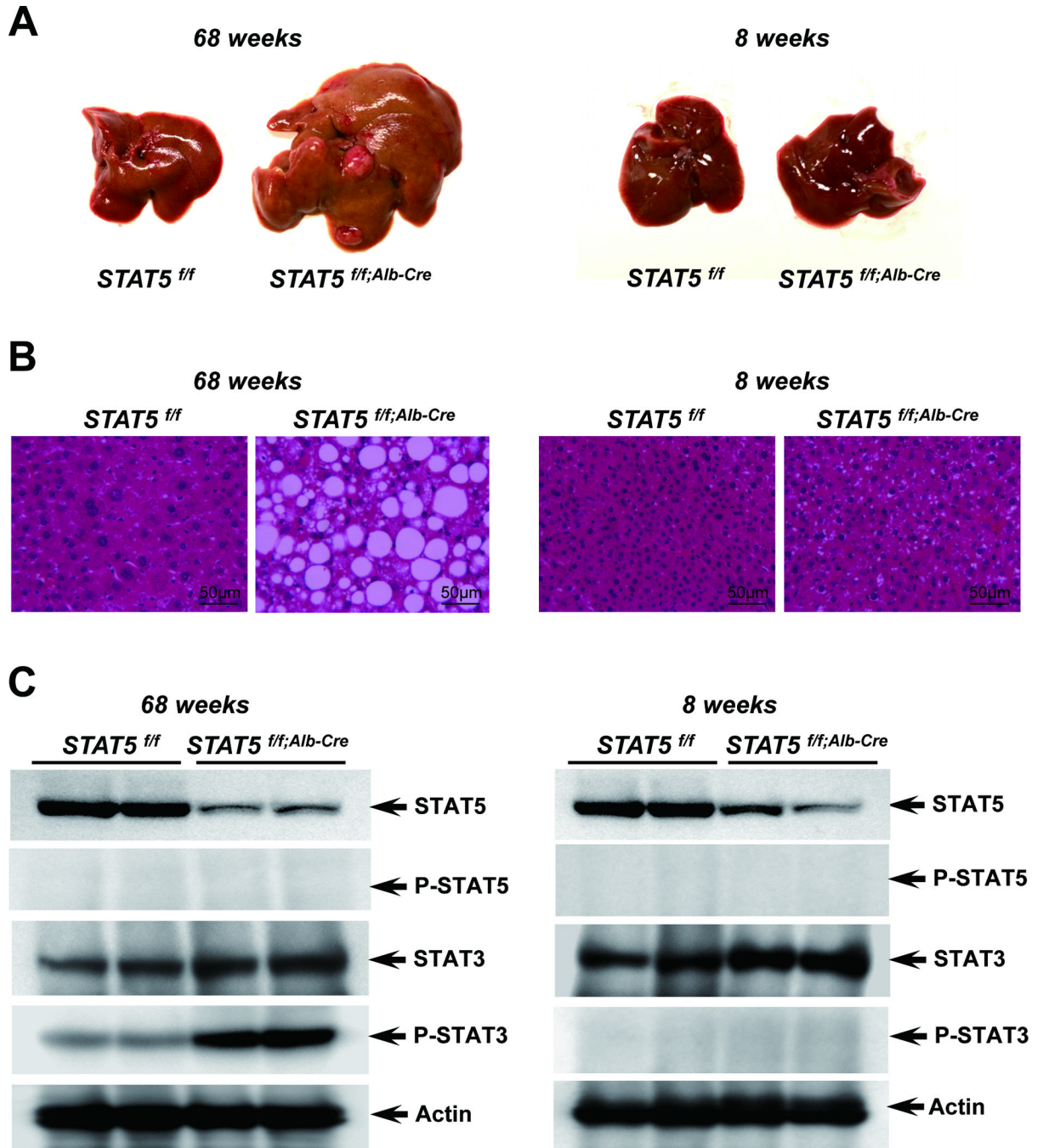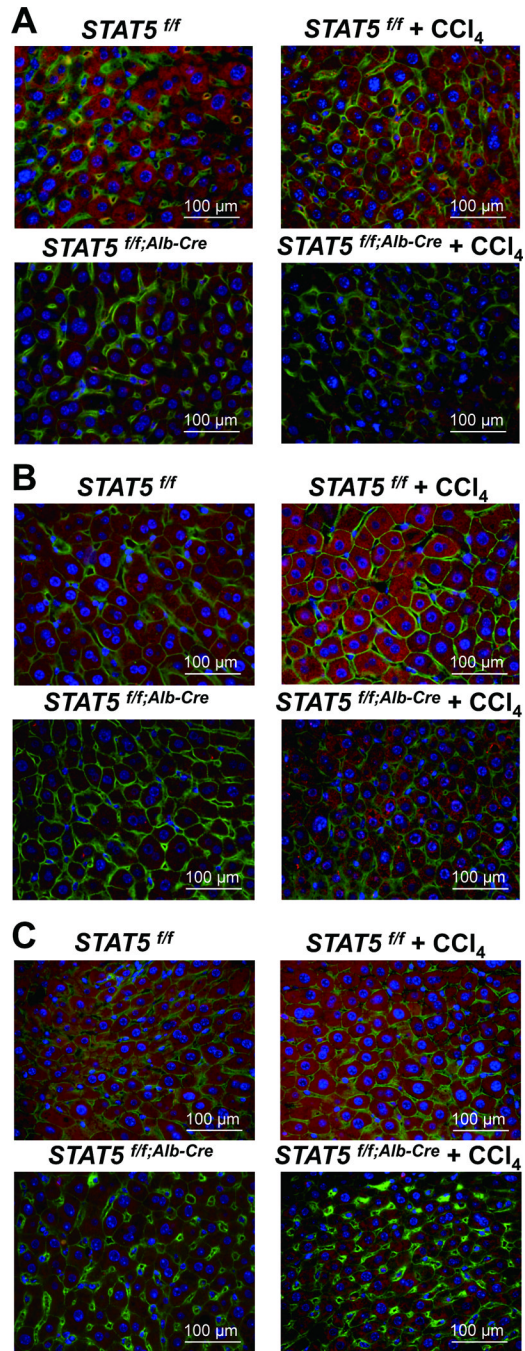
Figure 4.
Loss of STAT5 induces development of tumor in *Stat5^{f/f;Alb-Cre}* mice. (A) Liver of *Stat5^{f/f} and Stat5^{f/f;Alb-Cre}* mice at 17 months (left) and 2 months (right). (B) Hematoxylin and eosin (H&E) staining of liver sections from *Stat5^{f/f} and Stat5^{f/f;Alb-Cre}* mice. (C) Level of STAT5, p-STAT5, STAT3 and p-STAT3 in liver tissues from *Stat5^{f/f} and Stat5^{f/f;Alb-Cre}* mice. Expression of STAT5, p-STAT5, STAT3 and p-STAT3 was determined by western blotting.
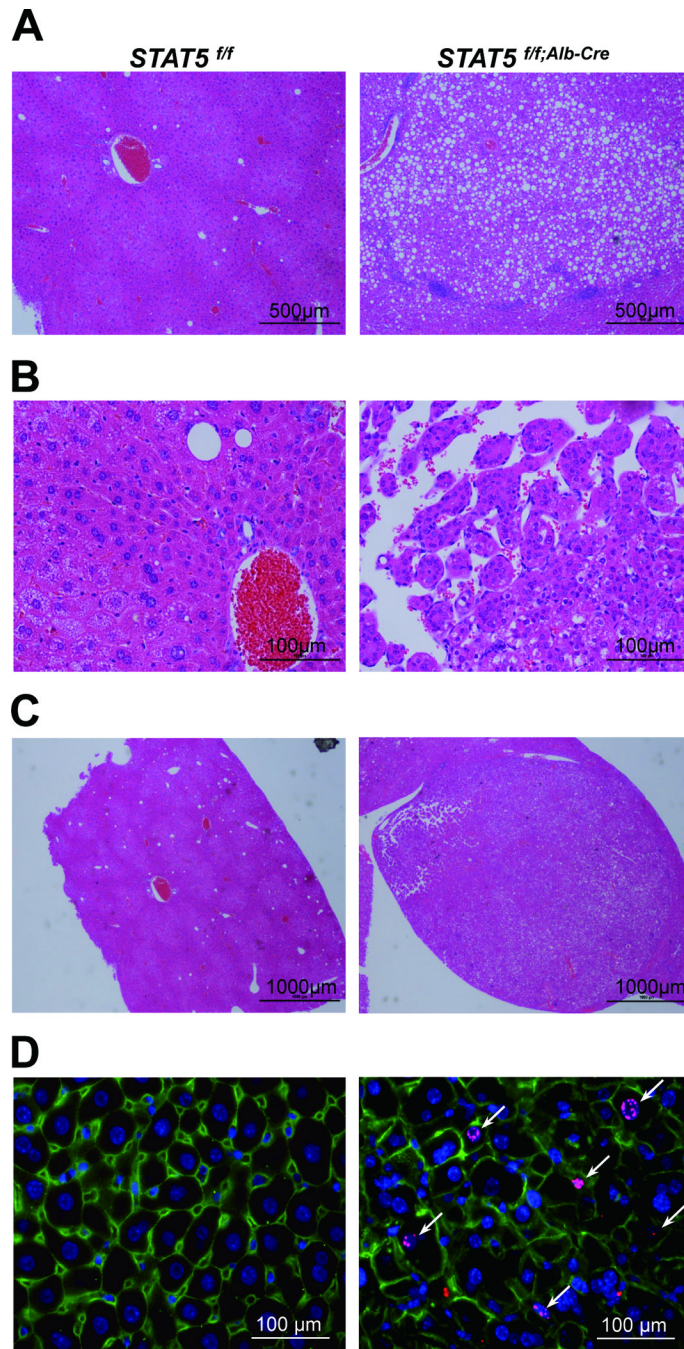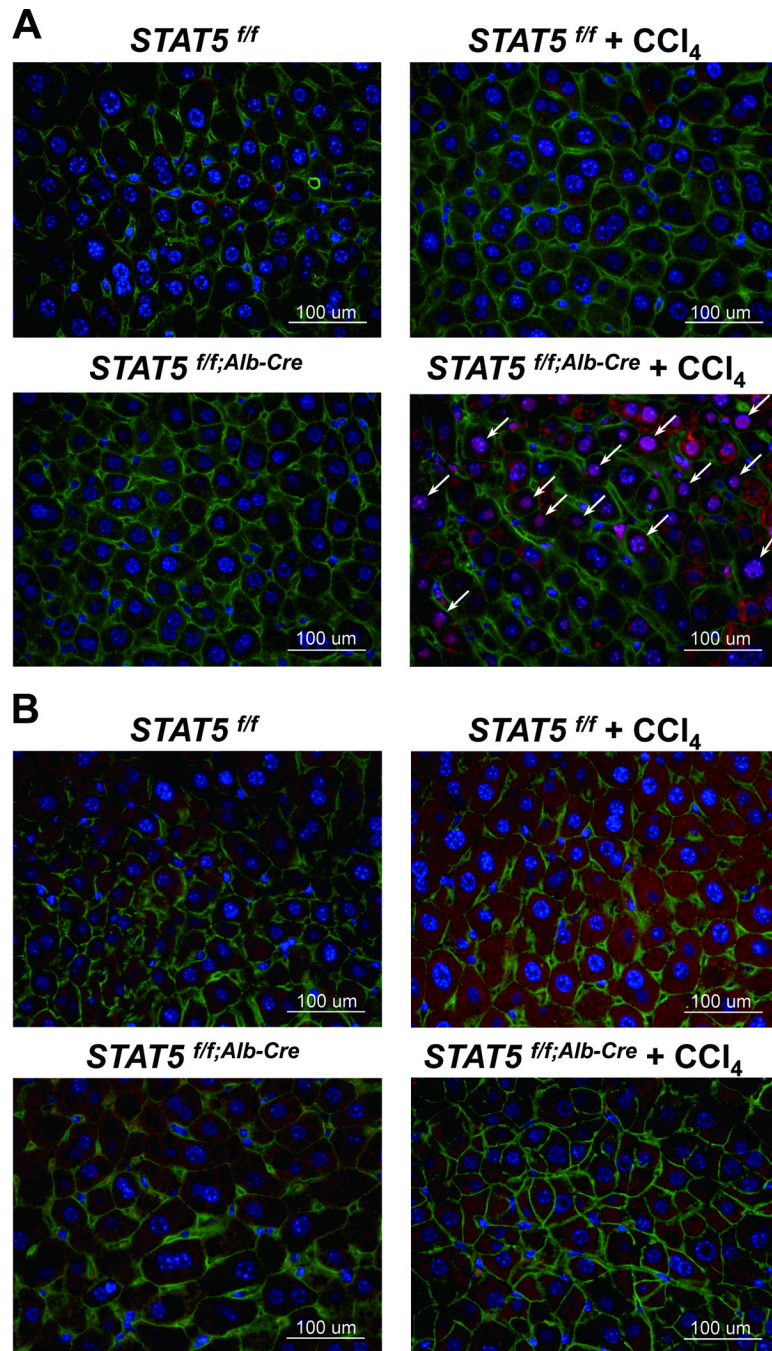
Figure 5.
Histological analyses and immunostaining of phospho-Histone H3 in liver tissue from *Stat5^{f/f} and Stat5^{f/f;Alb-Cre}* mice. (A–C) Hematoxylin and eosin (H&E) staining of liver sections from *Stat5^{f/f} and Stat5^{f/f;Alb-Cre}* mice at 17 months of age. Hepatosteatosis (A) and hepatocellular carcinoma (HCC) (B) were only observed in liver-specific *Stat5*-null mice. Nodules were also observed only in liver-specific *Stat5*-null mice (C). (D) Liver tissue from 17 months old *Stat5^{f/f} and Stat5^{f/f;Alb-Cre}* mice was harvested and analyzed for phospho-Histone H3 using immunofluorescence staining with anti-phospho-Histone H3 (red), anti-β-catenin (green) antibodies and DAPI (blue).
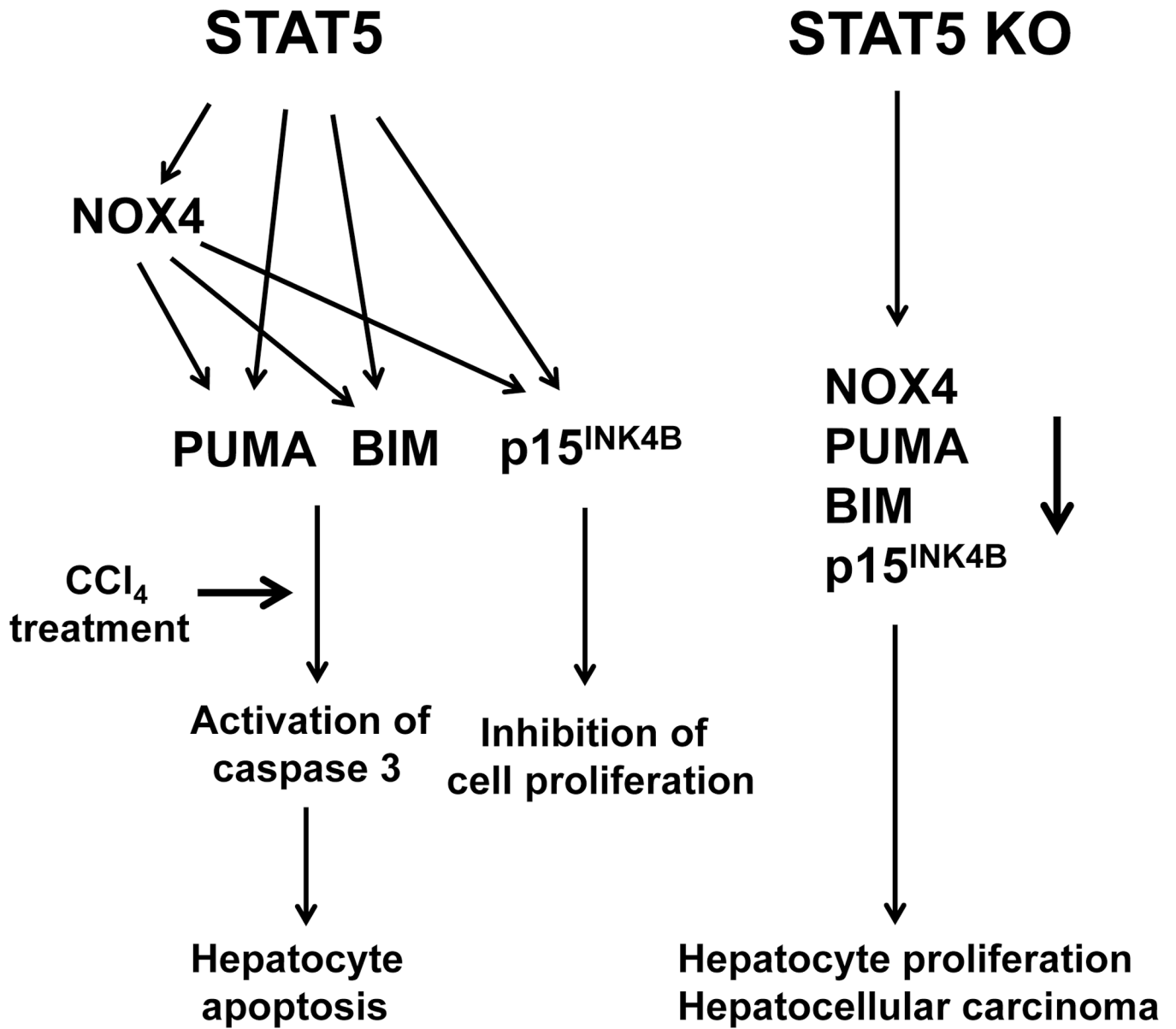
Figure 6.
Immunostaining of NOX4, PUMA and BIM in *Stat5$^{f/f}$ and Stat5$^{f/f;Alb-Cre}$* mice injected with CCl$_4$. (A–C) Liver tissue from *Stat5$^{f/f}$ and Stat5$^{f/f;Alb-Cre}$* mice was harvested after 12 weeks of CCl$_4$ injection and analyzed for expression of NOX4 (A), PUMA (B) and BIM (C) using immunofluorescence staining with anti-NOX4 (red), anti-PUMA (red), anti-BIM (red), anti-β-catenin (green) antibodies and DAPI (blue).

Figure 7.
Immunostaining of Ki-67 and cleaved caspase-3 in $Stat5^{f/f}$ and $Stat5^{f/f;Alb-Cre}$ mice injected with CCl$_4$. (A) Liver tissue from $Stat5^{f/f}$ and $Stat5^{f/f;Alb-Cre}$ mice was harvested after 12 weeks of CCl$_4$ injection and analyzed for Ki-67 using immunofluorescence staining with anti-Ki-67 (red), anti-β-catenin (green) antibodies and DAPI (blue). (B) Liver tissue from $Stat5^{f/f}$ and $Stat5^{f/f;Alb-Cre}$ mice was harvested after 12 weeks of CCl$_4$ injection and analyzed for cleaved caspase-3 using immunofluorescence staining with anti-cleaved caspase-3 (red), anti-β-catenin (green) antibodies and DAPI (blue).

Figure 8.
Proposed model of STAT5-regulated apoptosis in hepatocytes. Previous studies have shown that liver-specific STAT5-null mice develop hepatosteatosis and HCC upon treatment with CCl_4. STAT5 regulates key cell cycle inhibitor and apoptotic genes. STAT5 directly activates the genes encoding NOX4, PUMA and BIM and the cell cycle inhibitor p15[INK4B]. NOX4 can also control PUMA, BIM and p15[INK4B]. We propose that loss of STAT5 induces hepatocyte proliferation and HCC upon CCl_4 challenge as a result of decreased levels of PUMA, BIM and p15[INK4B].